Journal of Hazardous Materials 189 (2011) 40–47

Contents lists available at ScienceDirect

Journal of Hazardous Materials

journal homepage: www.elsevier.com/locate/jhazmat

Photocatalytic ozonation of dimethyl phthalate with TiO_2 prepared by a hydrothermal method

Yuan Jing, Laisheng Li*, Qiuyun Zhang, Ping Lu, Peihong Liu, Xianghong Lü

School of Chemistry & Environment, South China Normal University, Guangzhou 510006, China

ARTICLE INFO

Article history:
Received 24 March 2010
Received in revised form
30 November 2010
Accepted 27 January 2011
Available online 3 March 2011

Keywords:
TiO_2
A hydrothermal method
Dimethyl phthalate
Photocatalytic ozonation
Kinetics

ABSTRACT

TiO_2 was prepared by a hydrothermal method at a low temperature and used to degrade and mineralize dimethyl phthalate (DMP). TiO_2 was characterized by XRD, TEM, BET and UV–vis techniques. The characteristics of TiO_2 prepared by a hydrothermal method (h-t TiO_2) included a good crystalline anatase phase, greater surface area, stronger absorption to UV light wavelength and lower agglomeration than TiO_2 prepared by a classic sol–gel method (s–g TiO_2). The photocatalytic activity of h-t TiO_2 prepared under optimal hydrothermal condition (180 °C for 10 h) was 2.5 times higher than that of s–g TiO_2 in degrading DMP. The process of photocatalysis combined with UV irradiation and ozonation (TiO_2/UV/O_3) considerably improved the mineralization and degradation of DMP compared to photocatalysis combined with UV irradiation (TiO_2/UV), ozonation combined with UV irradiation (UV/O_3), and ozonation alone (O_3). A kinetic study showed the mineralization in TiO_2/UV/O_3 followed the Langmuir–Hinshelwood model.

1. Introduction

Phthalate esters (PAEs) are widely used as plasticizers, primarily in the production of polyvinyl chloride resins. The short-chained esters such as dimethyl phthalate (DMP) are the most frequently identified PAEs in diverse environmental samples, including surface marine water, freshwater and sediments [1]. Its toxic properties are of particular concern due to its high bioaccumulation rate (range from 100 to 3000) in different organisms [2]. It is also an endocrine disruptor [3]. DMP is a relatively stable compound in natural environment, its hydrolysis half-life is estimated to be about 20 years [4].

Photocatalytic processes have received much attention in recent years, particularly for their complete destruction, or mineralization of toxic and non-biodegradable compounds to carbon dioxide and inorganic constituents in both water and gas phase [5]. Among the photocatalysts applied, nanosized TiO_2 has proven to be an excellent catalyst in the photocatalytic degradation of organic pollutants because it is an effective, photostable, reusable, inexpensive, nontoxic and easily available catalyst [6].

For the fabrication of TiO_2, the sol–gel technique has been widely employed due to the low cost of the equipment required and the resulting high purity products. However, such high calcination temperatures will result in the increase in nanoparticle size and the decrease in specific surface area (increasing mass transfer limitations) [7]. To prepare highly photoactive nanocrystalline TiO_2 powders, a reasonable route would be to reduce the temperature of the phase transformation of amorphous to anatase [8,9]. The hydrothermal technique is a "soft solution chemical process", which facilitates the control of grain size, particle morphology, microstructure, phase composition, and surface chemical properties by adjusting experimental parameters such as temperature, pressure, process duration and the pH value of the solution [10,11]. In TiO_2-photocatalytic oxidation processes, oxygen is widely used as an additional oxidant, the disadvantage is the slow electron transfer from TiO_2 to O_2 [12]. Ozone is a powerful oxidant (E^0 = 2.07 V) and reacts with many compounds via direct or indirect reactions (mainly, $OH^\bullet$). Electrophilic attack by ozone molecules may occupy atoms with a negative charge density or double/triple bonds such as carbon–carbon. Indirectly, ozone can react by the free radicals ($OH^\bullet$) (E^0 = 2.80 V), which are powerful and nonselective oxidant, and can react with almost all organic compounds [13]. Therefore, it is necessary to develop more powerful oxidation methods for total mineralization of organic compounds. The combined ozonation and photocatalytic (Degussa P25 TiO_2) has been successfully used for the degradation of organic pollutants (such as pesticides, antibiotic sulfamethoxazole and toluene in waters) because a commercial Degussa P25 TiO_2 has high chemical stability, optical and electronic properties [14–16]. But the photocatalytic activity (by degrading acetone) of the prepared TiO_2 powders under the optimal hydrothermal conditions was three times more than that of Degussa P25 TiO_2 [8].

* Corresponding author. Tel.: +86 20 39310185; fax: +86 20 39310187.
E-mail addresses: llsh@scnu.edu.cn, llsh99@mails.tsinghua.edu.cn (L. Li).

0304-3894/$ – see front matter © 2011 Elsevier B.V. All rights reserved.
doi:10.1016/j.jhazmat.2011.01.132

Recently, there are a few publications on the ozonation of DMP to study its degradation and TOC removal with the presence of catalyst or UV radiation [17–23], such as the catalytic ozonation of DMP in the presence of heterogeneous Ru/Al_2O_3, Ru or Ce/AC (activated carbon) catalyst [17–19]. The results indicated that the mineralization of DMP during ozonation could be promoted by the use of Ru/Al_2O_3, Ru or Ce/AC catalyst because of improvement of mass transfer, but the preparation of Ru/Al_2O_3, Ru/AC catalyst is relatively expensive. And also AC (support) is easily oxidized by ozonation process, which results in decreasing of catalyst's activity with ozonation reaction time [24,25]. In addition, the catalytic ozonation (with high silica zeolites or Pt/Al_2O_3 as a catalyst) of DMP in the presence of UV radiation emitting principally at 254 nm studied [20–22]. Their results also indicated that the degradation and mineralization of DMP during ozonation could be promoted by UV radiation at 254 nm (a higher energy supply), but the preparation of the photocatalyst (high silica zeolites, porous polyoxotungstate/titania nanocomposites or Pt/Al_2O_3) is complicated and expensive [21–23].

In this study, the advantages of TiO_2 by a hydrothermal method were demonstrated. They include the higher surface area (increasing mass transfer) and photocatalytic activity by UV radiation emitting principally at 365 nm (a lower energy supply) compared to TiO_2 prepared by the classic sol–gel method, and excellent efficiency for photocatalytic ozonation to remove DMP.

2. Materials and methods

2.1. Catalyst preparation

Tetrabutyl titanate ($Ti(OC_4H_9)_4$, TBOT) was used as a titanium source. TBOT (13.2 ml) was added drop-wise to 130 ml pure water in a 250 ml beaker under continuous stirring for 30 min. Sol samples obtained by the hydrolysis reaction were transferred into a Teflon-lined stainless steel auto-clave. Hydrothermal reactions were conducted at different conditions. After a hydrothermal reaction, the white precipitates were washed five times with deionized water and ethanol, then dried in an oven at 80 °C for 10 h to obtain TiO_2 samples (labeled h-t TiO_2) [26].

For comparison, the other TiO_2 was produced by a classic sol–gel method. 100 ml of absolute alcohol, 20 ml of tetrabutyl titanate and 3 ml of glacial acetic acid were mixed as a solution at room temperature. Then it was added 4 ml deionized water, drop-wise with vigorous stirring. The mixed solution was aged for 48 h allowing formation of a xerogel, then dried in an oven at 80 °C for 10 h. The powder was calcined at 500 °C for 2 h, yielding TiO_2 (labeled s–g TiO_2).

2.2. Experimental set-up and process

A 1 l glass tubular photoreactor (h = 500 mm, φ_{in} = 60 mm) was employed for the photocatalytic oxidation experiments. A coaxial UV source comprised a 15 W UV lamp with wavelength 365 nm surrounded by a quartz thimble (30 mm diameter). 1.0 l DMP around 10 mg l^{-1} solution (pH = 5.5) and 1.0 g catalyst were added. Ozone was produced from pure oxygen (air flow rate = 1.0 L min^{-1}) by using a DHX-SS-03C ozone generator (made in China). Ozonized oxygen was continuously bubbled into the solution through a porous glass plate and flowed upward in the annular section. The excess ozone in the outlet gas was absorbed by a 5% $Na_2S_2O_3$ solution. Samples were taken at intervals to analyze DMP and total organic carbon (TOC) concentrations. $Na_2S_2O_3$ solution was used to stop the continuous ozonation reaction in the sample. The reaction temperature was remained at 25 °C in all experiments.

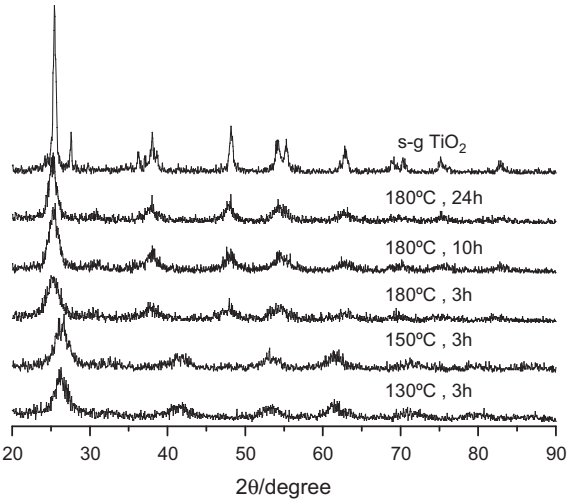

Fig. 1. XRD patterns of TiO_2 powders prepared at different conditions.

2.3. Catalyst characterization

The BET surface area was determined by nitrogen adsorption (Micromeritics ASAP 2020, USA). All the samples were degassed at 180 °C prior to nitrogen adsorption measurements. Grain size as well as the crystalline phase of TiO_2 was determined using an X-ray diffractometer (Y-2000, China) with a diffractometer employing Cu K radiation at a scan rate of 0.1° 2θ s^{-1}. The accelerating voltage and applied current were 15 kV and 20 mA, respectively. The morphology of the samples was visualized using transmission electron microscope (FEI-Tecnai 12, Holland). UV–vis diffuse reflection spectra were obtained using a UV–vis spectrophotometer (UV3150, Shimadzu, Japan).

2.4. Analytical methods

The concentration of DMP was determined by high performance liquid chromatography (Shimadzu, LC10A HPLC) with a UV detector (SPD-10AV) at 254 nm. A Discovery C18 column (250 mm × 4.6 mm) was used, and the analysis was carried out with a 70/30 (v/v) methanol/water mobile phase at a flow rate of 1.0 mL min^{-1}. Total organic carbon (TOC) was determined by a Shimadzu TOC-VCPH analyzer after filtration through 0.45 μm profiler.

3. Results and discussion

3.1. Catalyst characterization

3.1.1. XRD spectra

XRD was used to investigate the changes of the prepared TiO_2 powders. XRD patterns of h-t TiO_2 at different conditions and s–g TiO_2 were compared in Fig. 1. It can be seen that the s–g TiO_2 primarily consisted of polycrystalline anatase structures, which had a little rutile content after calcining at 500 °C. The h-t TiO_2 totally appears anatase phase. Usually, TiO_2 phase transformation temperature from the amorphous to anatase phase is higher than 400 °C during the calcination. However, h-t TiO_2 can transform from amorphous to the anatase phase at a low temperature (for example, <200 °C). It can be concluded that a hydrothermal process enhances the phase transformation of TiO_2 powders from amorphous to anatase at a low temperature due to a non-equilibrium pressure environment. The average crystallite size of TiO_2 (180 °C, 10 h) was calculated by Scherrer's equation using the full width at half maximum of the X-ray diffraction peaks. The crystallite size

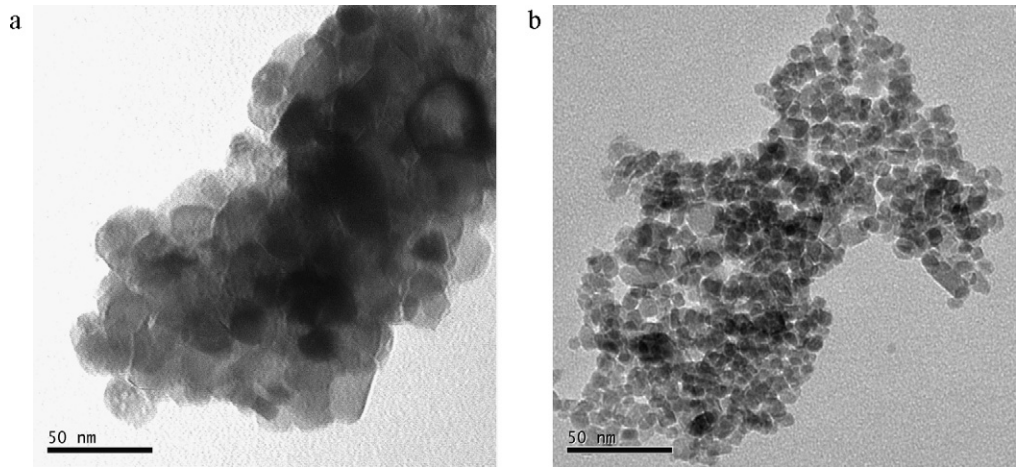

Fig. 2. TEM images of s–g TiO_2 (a) and h-t TiO_2 (b).

of h-t TiO_2 was 8.4 nm which was smaller than 11.7 nm of sol–gel TiO_2. Using a hydrothermal method, nanoparticle size increase followed by high shrinkage or collapse of the mesostructure at a high temperature can be avoided [7]. It can be seen that TiO_2 samples after hydrothermal treatment at 100 °C (a), 150 °C (b) and 180 °C (c) for 3 h appear totally anatase phase. Observation shows that the peak intensities of anatase steadily become stronger and the width of the diffraction peak of anatase ($2\theta = 25.4°$) slightly becomes narrower with increasing hydrothermal temperature, indicating the formation of greater TiO_2 crystallites and the enhancement of crystallization of TiO_2 [27]. The effect of hydrothermal time on phase structures of TiO_2 powders at 180 °C was also displayed in Fig. 1. It can be seen that the peak intensities of anatase increase and the width of the (1 0 1) plane diffraction peak of anatase become narrower with increasing hydrothermal time.

3.1.2. TEM image

TEM photographs of h-t TiO_2 at 180 °C for 10 h and s–g TiO_2 are displayed in Fig. 2. It could be observed from Fig. 2(a) that the nanocrystallite of s–g TiO_2 showed an agglomerated status. The crystallization of titania by a sol–gel method takes place at high temperatures (400–600 °C), and is accompanied with high shrinkage or collapse of the mesostructure and is eventually followed by the agglomeration of nanoparticles [7]. Whereas it can be observed from Fig. 2 (b) that the primary particles of h-t TiO_2 were relatively uniform and their sizes were in agreement with the values determined by XRD analysis. Avoiding the calcination at a high temperature by a hydrothermal method, the agglomeration of TiO_2 powders can be reduced.

3.1.3. BET surface areas

The surface area, pore volume and pore size of TiO_2 are provided by nitrogen adsorption. The surface area and pore volume of h-t TiO_2 prepared at 180 °C for 10 h were 189.7 $m^2\,g^{-1}$ and 0.4 $cm^3\,g^{-1}$ which were 2.5 and 3.5 times more than those of s–g TiO_2. Increasing photocatalyst surface area affords greater opportunity for contact with organic pollutants and the hole-electron pairs production radiated by UV lamp. The h-t TiO_2 displayed larger surface areas due to diminished agglomeration which decreases the specific surface area [28–30].

3.1.4. UV–vis diffuse reflectance spectra

Fig. 3 shows the UV–vis diffuse reflectance spectra of h-t TiO_2 (180 °C, 10 h) and s–g TiO_2. They show a strong absorption in the region of UV light, which typically optical characteristic is held by a semiconductor. Further observation shows h-t TiO_2 has the

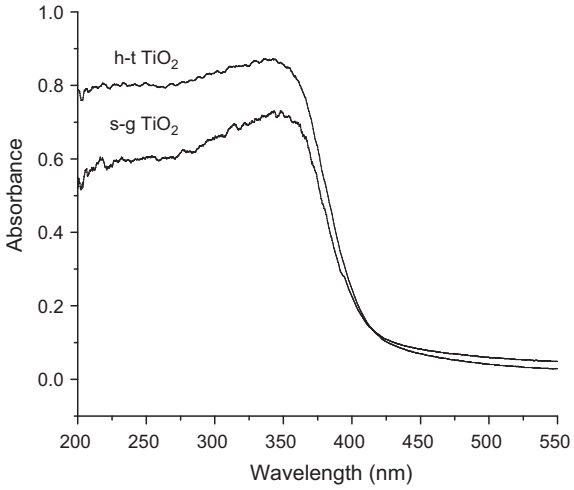

Fig. 3. The diffuse reflectance spectra of h-t TiO_2 and h-t TiO_2.

stronger reflectance to visible light and stronger absorption to UV light. It combined with the anatase crystal form, smaller crystal grains and larger surface area increase the photocatalytic activity.

3.2. The photocatalytic activity evaluation of TiO_2 by a hydrothermal method

Hydrothermal temperature and time were two major factors in a hydrothermal process. Fig. 4 shows the dependence of photocatalytic activity on hydrothermal temperature and time. Fig. 4(a) illustrates that TiO_2 powders prepared at 100 °C for 3 h exhibited the lower photocatalytic activity for photocatalytic degradation of DMP. Firstly, DMP removal rate was increased with hydrothermal temperature, and reached a maximum value of 50.7% at 180 °C (60 min), and then decreased with increasing hydrothermal temperature. The enhancement of photocatalytic activity at an elevated hydrothermal temperature can be ascribed to an obvious improvement in relative anatase crystallinity [8]. Fig. 4(b) shows the effect of hydrothermal time on photocatalytic activity of h-t TiO_2. It can be seen that DMP removal rate increases with hydrothermal time. The enhancement of photocatalytic activity at a longer hydrothermal time is due to anatase crystallinity reinforcement [8]. At 10 h, DMP removal rate at 60 min reaches the highest (58.9%). With further increasing hydrothermal time, the photocatalytic activity decreases, which is due to the sharp decrease in BET specific surface

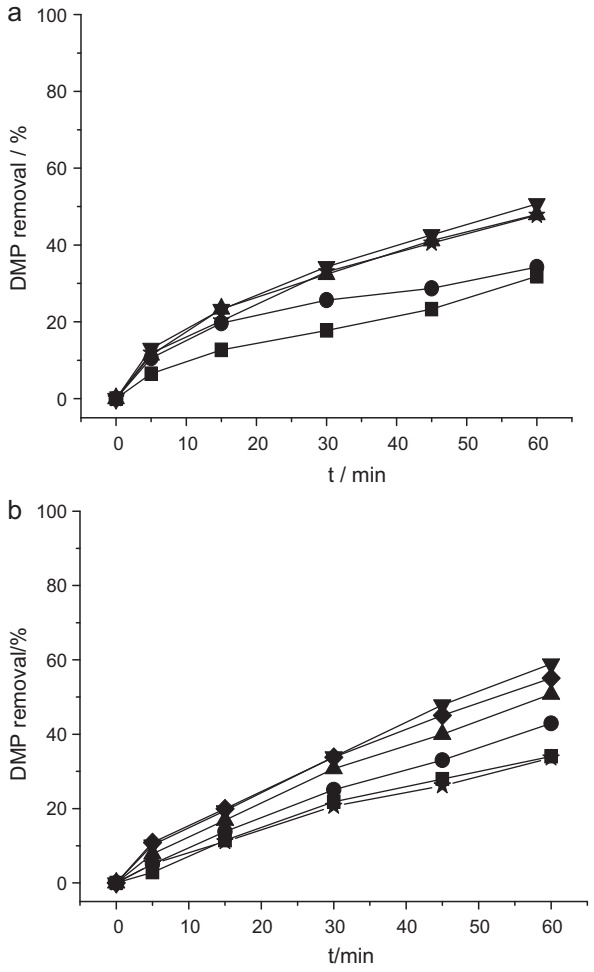

Fig. 4. The photocatalytic activity of h-t TiO_2 for DMP degradation at different hydrothermal conditions. (a) h-t TiO_2 at different hydrothermal temperature after 3 h hydrothermal time: (■) 100 °C; (●) 120 °C; (▲) 150 °C; (▼) 180 °C; (★) 200 °C. (b) h-t TiO_2 at different hydrothermal time under 180 °C hydrothermal temperature: (■) 1 h; (●) 3 h; (▲) 5 h; (▼) 10 h; (♦) 24 h; (★) s–g TiO_2.

areas and hydroxyl content. So an optimal hydrothermal condition (180 °C for 10 h) for photocatalytic activity of h-t TiO_2 was determined.

The difference of photocatalytic activity between h-t TiO_2 prepared at 180 °C for 10 h and s–g TiO_2 is obvious. DMP removal by TiO_2/UV/O_2 process was 62.1% at 60 min by using h-t TiO_2, while only 33.6% with s–g TiO_2. DMP removal rate constants (k) were calculated based on a first-order reaction kinetic with R^2 values greater than 0.99. The rate constant with h-t TiO_2 was 0.0164 min^{-1}, 2.5 times more than that of s–g TiO_2. Generally, the larger specific surface area of h-t TiO_2 facilitates the absorption and utilization of UV light, which is also essential for photocatalytic degradation [31]. Besides, it is commonly accepted that the smaller crystalline size means more powerful redox ability because of the quantum-size effect [32]. The smaller crystalline sizes are also beneficial for the separation of photogenerated hole and electron pairs. These features should slow the rate of e^-–h+ recombination and increase photocatalytic activity [33]. Therefore, it would be reasonable to explain the higher photocatalytic activity of h-t TiO_2.

3.3. Degradation and mineralization of DMP in different oxidation processes

Fig. 5 provides the degradation curves of DMP as a function of reaction time in the O_3, UV/O_2, TiO_2/UV/O_2, TiO_2/O_3, UV/O_3 and

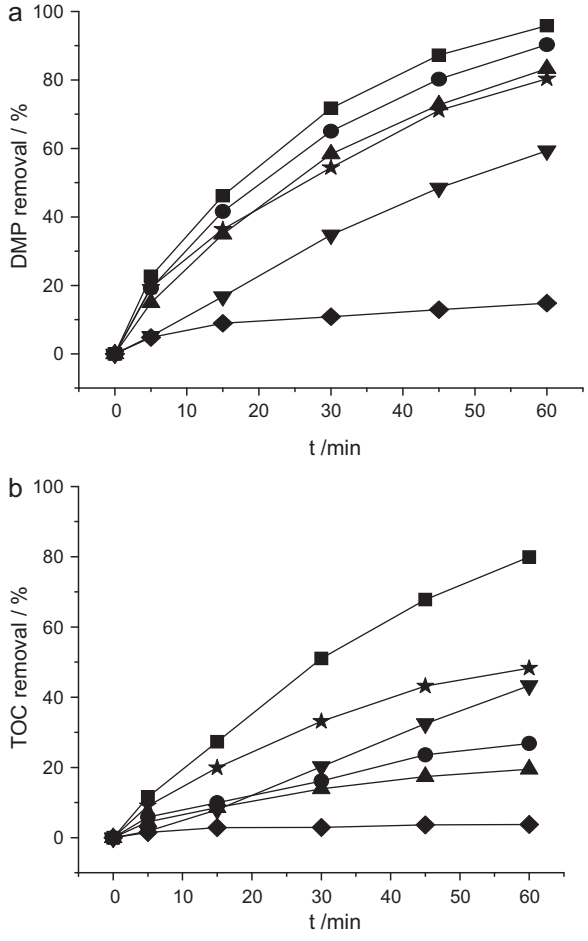

Fig. 5. DMP degradation and TOC removal by different processes: (■) TiO_2/UV/O_3; (●) UV/O_3; (▲) O_3; (▼) TiO_2/UV/O_2; (♦) UV/O_2; (★) TiO_2/O_3.

TiO_2/UV/O_3 processes with 20 mg h^{-1} O_3 dosage. The h-t TiO_2 prepared at 180 °C for 10 h was used in all processes. The UV/O_2 process gave 14.8% DMP removal at 60 min, indicating that UV irradiation had a weak effect on DMP degradation. DMP molecules absorb radiation with the absorbance maximum at 227 nm, but the applied light source mainly emits radiation approximately 365 nm and this is the reason that DMP slowly degraded within UV/O_2 process [34]:

$$\mathrm{DMP} \xrightarrow{h\nu} \mathrm{products} \quad (1)$$

Adding ozone into the reaction, DMP degradation rate was improved. For example, DMP removal rate by O_3, UV/O_3, and TiO_2/UV/O_3 processes were 83.3%, 90.3%, 95.8%, respectively, at 60 min oxidation reaction, whereas DMP removal rate was only 59.3% at 60 min in TiO_2/UV/O_2 process. In TiO_2/O_3 process, the presence of TiO_2 did not improve DMP removal (80.4% at 60 min oxidation time), which was lower than that (83.3% at 60 min oxidation time) in ozone process, because the presence of TiO_2 nano particles slows the transference of ozone in water. However, TOC removal was different from DMP degradation. TiO_2/UV/O_3 process provided the best performance and O_3 alone process presented the worst in TOC removal. TOC removal rate of DMP by the O_3, UV/O_3, TiO_2/O_3 and TiO_2/UV/O_3 processes were 19.5%, 26.9%, 48.3%, 79.9%, respectively, at 60 min oxidation reaction. The presence of TiO_2 significantly increased TOC removal rate, because TiO_2 was an extensive useful catalyst and adsorbed oxygen into the form of superoxide ion (O^{2-}) which in water promotes the decomposition

of ozone into free radicals [35,36]:

$$O_2 + H_2O \xrightarrow{TiO_2} e^- + O_2^- + H^+ \quad (2)$$

$$O_3 + O_2^- \rightarrow O_3^- + O_2 \quad (3)$$

$$O_3^- + H^+ \rightarrow HO^\bullet \quad (4)$$

An obvious difference between O_3 and UV/O_3 processes is that the combination of photodegradation with ozone has a synergistic effect in mineralization but it was not shown in DMP removal. The UV light irradiation can accelerate the decomposition of ozone, the selective oxidation of DMP reduced [13], the consequence of the photodegradation of ozone molecules by UV irradiation where ozone absorbs some of the incoming photons, leads to its degradation to atomic O (1D). It then reacts with water forming H_2O_2. In the subsequent reactions, new reactive species are formed from H_2O_2, and this enhances the degradation of the organic substrate [34]:

$$O_3 \xrightarrow{h\nu} O(^1D) + O_2 \quad (5)$$

$$O\ (^1D) + H_2O \rightarrow H_2O_2 \quad (6)$$

$$H_2O_2 + DMP \rightarrow \text{products} \quad (7)$$

$$H_2O_2 \rightarrow HO^\bullet \quad (8)$$

DMP removal ratio can reach 83.3% by using O_3 alone process, but TOC removal ratio is only 19.5%, it presents that O_3 ($E^0 = 2.07$ V) directly oxidizes DMP into some small molecule intermediates, which are not easy to be mineralized furthermore, some organic acids are produced in the oxidation process of aromatics, such as formic acid and oxalic acid. Ozonation alone can only achieve a very limited mineralization of formic and oxalic acids because their ozonation rate constants are 5 and $<4 \times 10^{-2}\ M^{-1}\ s^{-1}$ in the acidic pH, respectively [37]:

$$DMP + O_3 \rightarrow \text{products} \quad (9)$$

But in $TiO_2/UV/O_2$ process, despite DMP removal ratio is only 59.3%, TOC removal ratio can reach 43.3%, because TiO_2 absorbs light at wavelength <385 nm with the corresponding production of holes and electrons. In the aqueous solutions, oxidation of water to hydroxyl radical by the hole appears to be the predominant pathway and in aerated aqueous suspensions, the electrons promote the reduction of dissolved oxygen to superoxide anion. The hydroxyl radicals and the lesser extent superoxide anion (O_2^-) can act as oxidants, ultimately leading to mineralization of organic compounds [14]:

$$TiO_2 \xrightarrow{h\nu} h^+ + e^- \quad (10)$$

$$h^+ + H_2O \rightarrow HO^\bullet \quad (11)$$

$$e^- + O_2 \rightarrow O^{2-} \quad (12)$$

$$HO^\bullet + DMP \rightarrow CO_2 + H_2O \quad (13)$$

$$O^{2-} + DMP \rightarrow CO_2 + H_2O \quad (14)$$

TOC removal curves of these four processes (including UV/O_3, $TiO_2/UV/O_2$, TiO_2/O_3 and $TiO_2/UV/O_3$) approximately follow first-order kinetics, the reaction can be simply described by $dTOC/dt = -kt$. The rate constant for $TiO_2/UV/O_3$ was 0.0265 min^{-1} which was 2.8 times, 2.4 times and 5.2 times more than those for $TiO_2/UV/O_2$, TiO_2/O_3 and UV/O_3.

It is clearly seen that $TiO_2/UV/O_3$ process had an excellent removal efficiency in both DMP and TOC, and synergistic effect of its TOC removal was proved by those of UV/O_3 and $TiO_2/UV/O_2$ processes. $TiO_2/UV/O_3$ process was an efficient technique for degradation and mineralization of DMP. Ozone, a stronger oxidant than oxygen, is more easily reduced by a photo-generated conduction electron from TiO_2 (step 9), thus it can effectively prevent the recombination of holes and electrons [38]:

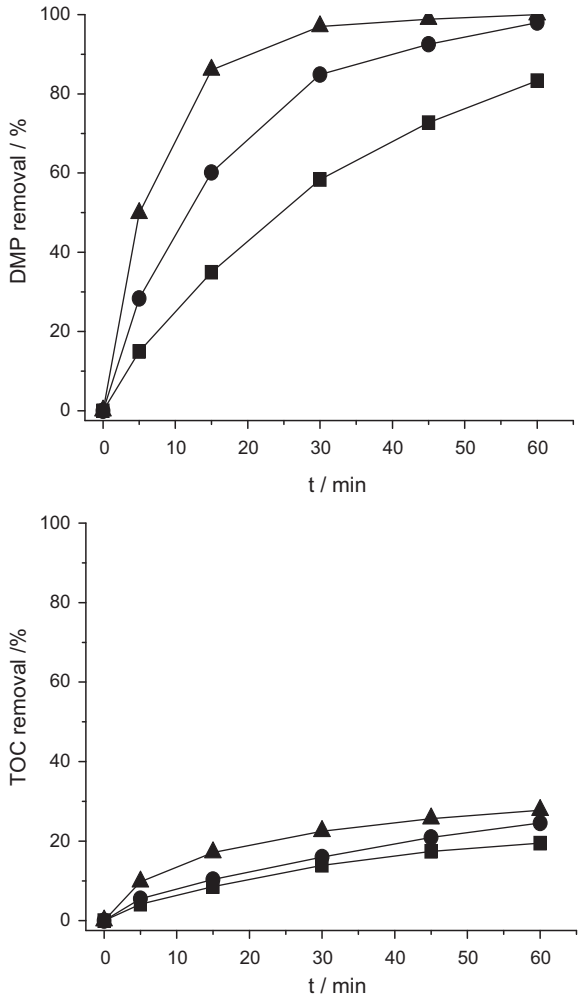

Fig. 6. Degradation of DMP and TOC removal with different ozone dosage in O_3 alone processes: (■) 20 mg h^{-1}; (●) 50 mg h^{-1}; (▲) 100 mg h^{-1}.

$$O_3 + e^- \rightarrow O_3^- \quad (15)$$

Also, ozone absorbs UV radiation, generating more hydroxyl radicals, which enhance degradation of the organic substrate (steps 5–8) [34,39]. Moreover, molecular oxygen accepts the photogenerated electron (step 12), a resulting superoxide radical anion can react with ozone to give a hydroxyl radical in the subsequent steps [34]:

$$O_2^- + O_3 \rightarrow O_3^- + O_2 \quad (16)$$

$$O_3^- + H^+ \rightarrow HO_3^\bullet \quad (17)$$

$$HO_3^\bullet \rightarrow O_2 + HO^\bullet \quad (18)$$

3.4. Effect of ozone dosage on degradation and mineralization of dimethyl phthalate in different oxidation processes

To determine the effect of the ozone dosage on DMP removal efficiency in different oxidation processes, a series of experiments were carried out by varying ozone dosage from 20 to 100 mg h^{-1}. Fig. 6 indicates that the degradation rate of DMP appears to increase rapidly with ozone concentration in O_3 process alone. For example, DMP removal rate improved from 58.3% to 97.1% as the ozone concentration increased from 20 mg h^{-1} to 100 mg h^{-1} at 30 min.

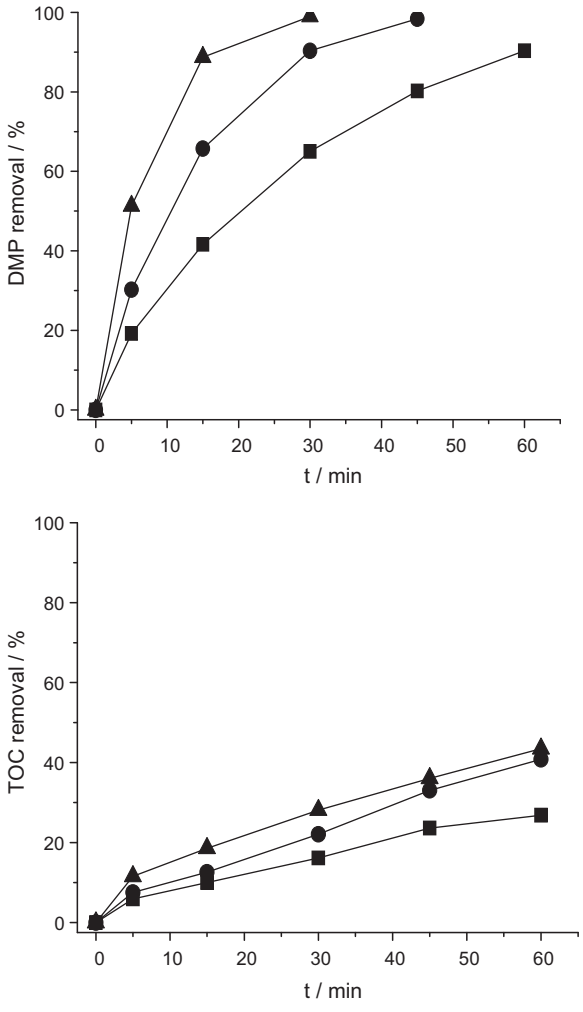

Fig. 7. Degradation of DMP and TOC removal with different ozone dosage in UV/O_3 process: (■) 20 mg h^{-1}; (●): 50 mg h^{-1}; (▲) 100 mg h^{-1}.

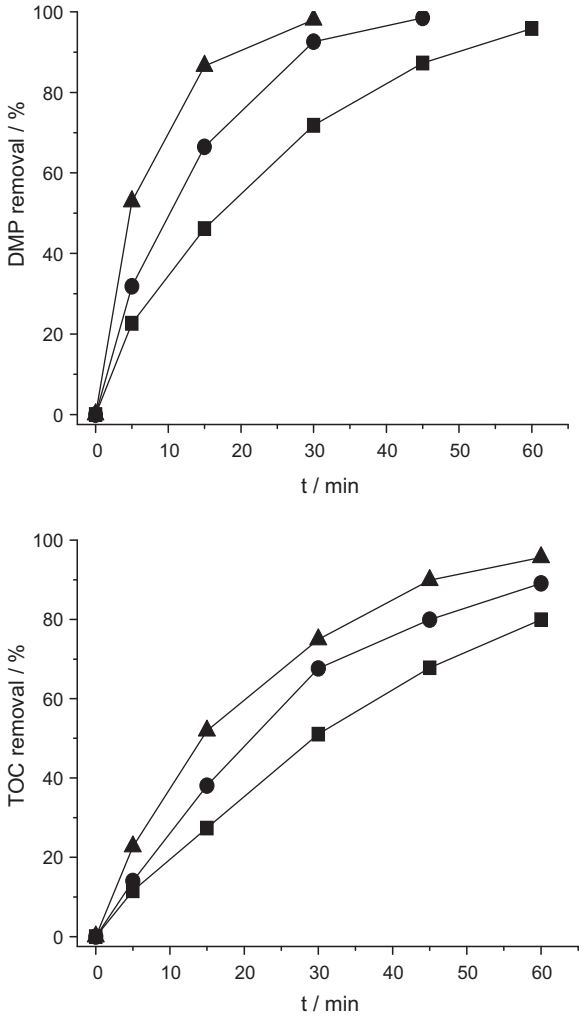

Fig. 8. Degradation of DMP and TOC removal with different ozone dosage in TiO_2/UV/O_3 process: (■) 20 mg h^{-1}; (●) 50 mg h^{-1}; (▲) 100 mg h^{-1}.

However, TOC removal rate was much slower than the degradation rate. At 100 mg h^{-1} ozone dosage, DMP can be almost eliminated by ozone process alone within 30 min, but TOC removal rate at 60 min was only 27.7%, which is only 3.2 (8.3)% higher than that at 50 (20) mg h^{-1}. DMP could be more quickly removed with increasing ozone dosage, but its TOC removal reduction was immediately declined.

Fig. 7 illustrates that both DMP and TOC removal rates in UV/O_3 process increased compared to O_3 process alone. It is due to the hydroxyl radicals generated in UV/O_3 process [39]. However, the presence of UV does not greatly improve DMP degradation compared to ozonation alone (Fig. 7). The effect of ozone dosage in the UV/O_3 process is similar to that in O_3 process alone. The more ozone dosage increased the degradation of DMP but only slightly improved TOC removal. The maximum TOC removal rate was 43.5%, just 2.6 (16.6) % higher than that at 50 (20) mg h^{-1}, indicating that enhanced ozone concentration did not generate significantly more $OH^{\bullet}$ in UV/O_3 process.

The degradation and mineralization of DMP in TiO_2/UV/O_3 process are presented in Fig. 8. The effect of ozone dosage on the degradation of DMP was the same as those in O_3 and UV/O_3 processes. DMP removal was quickly increased with ozone dosage. However, the increase of ozone concentration considerably improved TOC removal. TOC removal rate at 45 min was 89.9% with 100 mg h^{-1} ozone dosage which was 10.1 (22.1)% higher than that with 50 (20) mg l^{-1}. Thus ozone dosage played a major role in TOC removal rate in TiO_2/UV/O_3 process, as it can partake in reactions such as direct ozone reaction, ozone photolysis producing hydroxyl radicals, ozone reaction with elections to the superoxide ion radical [40]. Utilization of ozone in the process of TOC removal greatly improved compared with O_3 and UV/O_3 processes.

3.5. Kinetics of DMP mineralization in TiO_2/UV/O_3 process

The Langmuir–Hinshelwood model has been widely used to formulate the rate equations for the photocatalytic reaction of a surface-catalyzed reaction [41]. The model uses the following equation to determine the reaction rate (r), where r is the reaction rate (mg l^{-1} min^{-1}), k is the reaction rate constant (mg l^{-1} min^{-1}), and K is the Langmuir adsorption coefficient (mg^{-1} l):

$$r = -\frac{\mathrm{dTOC}}{\mathrm{d}t} = k\frac{K\mathrm{TOC}}{1 + K\mathrm{TOC}} \tag{19}$$

$$\frac{1}{r} = \frac{1}{k} + \frac{1}{kK\mathrm{TOC}} \tag{20}$$

A series of experiments for TOC removal from different initial concentrations of DMP were researched in TiO_2/UV/O_3 process with different ozone dosage (20 mg h^{-1}, 50 mg h^{-1}, 100 mg h^{-1}). TOC removal efficiency is presented in Fig. 9. Calculating the linear regression of TOC^{-1} and r^{-1} indicated that the kinetics of TOC removal by TiO_2/UV/O_3 process was completely fitted by

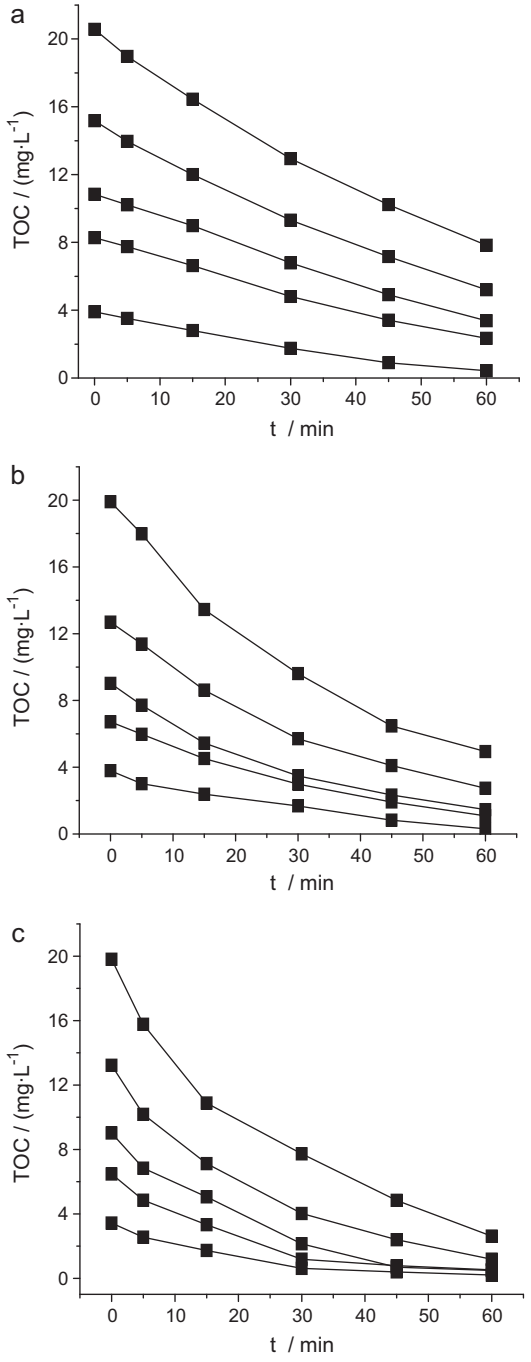

Fig. 9. TOC removal from different initial concentrations in $TiO_2/UV/O_3$ process with different ozone dosage: (a) 20 mg h^{-1}; (b) 50 mg h^{-1}; (c) 100 mg h^{-1}.

Table 1
The values of k and K in $TiO_2/UV/O_3$ process with different ozone dosage.

Ozone dosage (mg h^{-1})	k (mg l^{-1} min^{-1})	K (mg l^{-1})	R^2
20	0.42	0.0417	0.993
50	1.35	0.0112	0.999
100	4.23	0.0036	0.998

Langmuir–Hinshelwood model with the $R^2 > 0.99$. The values of k and K for the reaction system in $TiO_2/UV/O_3$ process were displayed in Table 1. These results indicated ozone may play a role for the mineralization of DMP. With increasing ozone dosage, the reaction rate constant was increased, but Langmuir adsorption coefficient was decreased. It is probably due to ozone competitive adsorption on the photocatalyst surface [42].

4. Conclusions

A TiO_2 photocatalyst was prepared by a hydrothermal method and characterized by XRD, TEM, UV–vis and BET techniques. Through a hydrothermal process at a low temperature instead of calcination, h-t TiO_2 displayed a good crystalline anatase phase, minimal agglomeration, plus smaller crystal sizes, stronger UV wavelength absorption and bigger surface area. Its photocatalytic activity for DMP degradation was 2.5 times more than that of TiO_2 produced by a sol–gel process.

The combination of ozone with photocatalytic oxidation was more efficient than other oxidation processes, especially for DMP mineralization. The rate constants in $TiO_2/UV/O_3$ process was 2.5 (5.2) times more than that in $TiO_2/UV/O_2$ (UV/O_3) process, implying a synergistic effect between the photocatalysis and ozonation.

For the degradation of DMP, ozone dosage played an important role in all the oxidation processes, DMP removal was rapidly increased with ozone dosage. In O_3 and UV/O_3 processes, with increasing ozone concentration, TOC removal was not as rapid as DMP degradation. However, in $TiO_2/UV/O_3$ process, the increase of ozone dosage considerably improved TOC removal. TOC removal at 45 min was 89.9% with 100 mg h^{-1} ozone dosage, 10.1 (22.1)% higher than that with a 50 (20) mg h^{-1} ozone dosage.

TOC removal in $TiO_2/UV/O_3$ process can be described by the Langmuir–Hinshelwood model. The reaction rate constant was increased with the ozone dosage, but Langmuir adsorption coefficient was decreased.

Acknowledgements

The authors are grateful for the financial support from the National Natural Science Foundation of China (contract No. 20977036) and the assistance of Dr. David E. Finlow from University of Tennessee at Chattanooga (a visiting professor of our university) with the English.

References

[1] W.E. Gledhill, R.G. Kaley, W.J. Adams, O. Hicks, P.R. Michael, V.W. Saeger, G.A. LeBlanc, Environmental safety assessment of butylbenzyl phthalate, Environ. Sci. Technol. 14 (1980) 301–305.
[2] C.A. Stables, D.R. Peterson, T.F. Parkerton, W.J. Adams, The environmental fate of phthalate esters: a literature review, Chemosphere 35 (1997) 667–749.
[3] B. Xu, N.Y. Gao, H.F. Cheng, S.J. Xia, M. Rui, D.D. Zhao, Oxidative degradation of dimethylphthalate (DMP) by UV/H_2O_2 process, J. Hazard. Mater. 162 (2009) 954–959.
[4] O. Bajt, G. Mailhot, M. Bolte, Degradation of dibutyl phthalate by homogeneous photocatalysis with Fe (III) in aqueous solution, Appl. Catal. B: Environ. 33 (2001) 239–248.
[5] L.C. Chen, F.R. Tsai, C.M. Huang, Photocatalytic decolorization of methyl orange in aqueous medium of TiO_2 and Ag–TiO_2 immobilized on γ-Al_2O_3, J. Photochem. Photobiol. A: Chem. 170 (2005) 7–14.
[6] A. Haarstrick, O.M. Kut, E. Heinzle, TiO_2-assisted degradation of environmentally relevant organic compounds in wastewater using a novel fluidized bed photoreactor, Environ. Sci. Technol. 30 (1996) 817–824.
[7] Q.R. Sheng, Y. Cong, S. Yuan, J.L. Zhang, M. Anpo, Synthesis of bi-porous TiO_2 with crystalline framework using a double surfactant system, Micropor. Mesopor. Mater. 95 (2006) 220–225.
[8] J.G. Yu, G.H. Wang, B. Cheng, M.H. Zhou, Effects of hydrothermal temperature and time on the photocatalytic activity and microstructures of bimodal mesoporous TiO_2 powders, Appl. Catal. B: Environ. 69 (2007) 171–180.
[9] H. Sakai, H. Kawahara, M. Shimazaki, M. Abe, Preparation of ultrafine titanium dioxide particles using hydrolysis and condensation reactions in the inner aqueous phase of reversed micelles: effect of alcohol addition, Langmuir 14 (1998) 2208–2212.
[10] Y.V. Kolen'ko, V.D. Maximov, A.V. Garshev, P.E. Meskin, N.N. Oleynikov, B.R. Churagulov, Hydrothermal synthesis of nanocrystalline and mesoporous titania from aqueous complex titanyl oxalate acid solutions, Chem. Phys. Lett. 388 (2004) 411–415.

[11] C. Su, C.M. Tseng, L.F. Chen, B.H. You, B.C. Hsu, S.S. Chen, Sol-hydrothermal preparation and photocatalysis of titanium dioxide, Thin Solid Films 498 (2006) 259–265.
[12] A. Sirisuk, C.G. HillJr, M.A. Anderson, Photocatalytic degradation of ethylene over thin films of titania supported on glass rings, Catal. Today 54 (1999) 159–164.
[13] L.S. Li, W.P. Zhu, L. Chen, P.Y. Zhang, Z.Y. Chen, Photocatalytic ozonation of dibutylphthalate over TiO_2 film, J. Photochem. Photobiol. A: Chem. 175 (2005) 172–177.
[14] R. Rajeswari, S. Kanmani, A study on synergistic effect of photocatalytic ozonation for carbaryl degradation, Desalination 242 (2009) 277–285.
[15] F.J. Beltrán, A. Aguinaco, J.F. García-Araya, A. Oropesa, Ozone and photocatalytic processes to remove the antibiotic sulfamethoxazole from water, Water Res. 42 (2008) 3799–3808.
[16] K.P. Yu, G.W.M. Lee, Decomposition of gas-phase toluene by the combination of ozone and photocatalytic oxidation process (TiO_2/UV, TiO_2/UV/O_3, and UV/O_3), Appl. Catal. B: Environ. 75 (2007) 29–38.
[17] J.B. Wang, Y.R. Zhou, W.P. Zhu, X.W. He, Catalytic ozonation of dimethyl phthalate and chlorination disinfection by-product precursors over Ru/AC, J. Hazard. Mater. 166 (2009) 502–507.
[18] L.S. Li, W.Y. Ye, Q.Y. Zhang, F.Q. Sun, P. Lu, X.K. Li, Catalytic ozonation of dimethyl phthalate over cerium supported on activated carbon, J. Hazard. Mater. 170 (2009) 411–416.
[19] Y.R. Zhou, W.P. Zhu, F.D. Liu, J.B. Wang, S.X. Yang, Catalytic activity of Ru/Al_2O_3 for ozonation of dimethyl phthalate in aqueous solution, Chemosphere 66 (2007) 145–150.
[20] B.S. Oh, Y.J. Jung, Y.J. Oh, Y.S. Yoo, J.W. Kang, Application of ozone, UV and ozone/UV processes to reduce diethyl phthalate and its estrogenic activity, Sci. Total Environ. 367 (2006) 681–693.
[21] Y.Y. Chen, N.C. Shang, D.C. Hsieh, Decomposition of dimethyl phthalate in an aqueous solution by ozonation with high silica zeolites and UV radiation, J. Hazard. Mater. 157 (2008) 260–268.
[22] C.C. Chang, C.Y. Chiu, C.Y. Chang, C.F. Chang, Y.H. Chen, D.R. Ji, Y.H. Yu, P.C. Chiang, Combined photolysis and catalytic ozonation of dimethyl phthalate in a high-gravity rotating packed bed, J. Hazard. Mater. 161 (2009) 287–293.
[23] L. Xu, X. Yang, Y.H. Guo, F.Y. Ma, Y.N. Guo, X. Yuan, M.X. Huo, Simulated sunlight photodegradation of aqueous phthalate esters catalyzed by the polyoxotungstate/titania nanocomposite, J. Hazard. Mater. 178 (2010) 1070–1077.
[24] M. Matheswarana, S. Balajia, S.J. Chunga, I.S. Moon, Studies on cerium oxidation in catalytic ozonation process: a novel approach for organic mineralization, Catal. Commun. 8 (2007) 1497–1501.
[25] X.K. Li, Q.Y. Zhang, L.L. Tang, P. Lu, F.Q. Sun, L.S. Li, Catalytic ozonation of p-chlorobenzoic acid by activated carbon and nickel supported activated carbon prepared from petroleum coke, J. Hazard. Mater. 163 (2009) 115–120.
[26] G.H. Wang, Hydrothermal synthesis and photocatalytic activity of nanocrystalline TiO_2 powders in ethanol–water mixed solutions, J. Mol. Catal. A: Chem. 274 (2007) 185–191.
[27] J.G. Yu, M.H. Zhou, B. Cheng, H.G. Yu, X.J. Zhao, Ultrasonic preparation of mesoporous titanium dioxide nanocrystalline photocatalysts and evaluation of photocatalytic activity, J. Mol. Catal. A: Chem. 227 (2005) 75–80.
[28] Y. Zhou, M. Antonietti, Synthesis of very small TiO_2 nanocrystals in a room-temperature ionic liquid and their self-assembly toward mesoporous spherical aggregates, J. Am. Chem. Soc. 125 (2003) 14960–14961.
[29] Z.J. Li, B. Hou, Y. Xu, D. Wu, Y.H. Sun, W. Hu, F. Deng, Comparative study of sol–gel-hydrothermal and sol–gel synthesis of titania-silica composite nanoparticles, J. Solid State Chem. 178 (2005) 1395–1405.
[30] J. Lin, Y. Lin, P. Liu, M.J. Meziani, L.F. Allard, Y.P. Sun, Hot-Fluid annealing for crystalline titanium dioxide nanoparticles in stable suspension, J. Am. Chem. Soc. 124 (2002) 11514–11518.
[31] J.M. Herrmann, Heterogeneous photocatalysis: fundamentals and applications to the removal of various types of aqueous pollutants, Catal. Today 53 (1999) 115–129.
[32] J.C. Yu, L.Z. Zhang, J.G. Yu, Direct sonochemical preparation and characterization of highly active mesoporous TiO_2 with a bicrystalline framework, Chem. Mater. 14 (2002) 4647–4653.
[33] T.Y. Peng, D. Zhao, K. Dai, W. Shi, K. Hirao, Synthesis of titanium dioxide nanoparticles with mesoporous anatase wall and high photocatalytic activity, J. Phys. Chem. B 109 (2005) 4947–4952.
[34] U. Černigoj, U.L. Štangar, P. Trebše, Degradation of neonicotinoid insecticides by different advanced oxidation processes and studying the effect of ozone on TiO_2 photocatalysis, Appl. Catal. B: Environ. 75 (2007) 229–238.
[35] F.J. Beltrán, F.J. Rivas, R. Montero-de-Espinosa, Catalytic ozonation of oxalic acid in an aqueous TiO_2 slurry reactor, Appl. Catal. B: Environ. 39 (2002) 221–231.
[36] A. Naydenov, D. Mehandjiev, Complete oxidation of benzene on manganese dioxide by ozone, Appl. Catal. A: Gen. 97 (1993) 17–22.
[37] L.S. Li, W.P. Zhu, P.Y. Zhang, Z.Y. Chen, W.Y. Han, Photocatalytic oxidation and ozonation of catechol over carbon black modified nano-TiO_2 thin films supported on Al sheet, Water Res. 37 (2003) 3646–3651.
[38] P.Y. Zhang, F.Y. Liang, G. Yu, Q. Chen, W.P. Zhu, A comparative study on decomposition gaseous toluene by O_3/UV, TiO_2/UV and O_3/TiO_2/UV, J. Photochem. Photobiol. A: Chem. 156 (2003) 189–194.
[39] C.S. Turchi, D.F. Ollis, Photocatalytic degradation of organic water contaminants: mechanisms involving hydroxyl radical attack, J. Catal. 122 (1990) 178–192.
[40] F.J. Beltrán, A. Aguinaco, J.F. García-Araya, Mechanism and kinetics of sulfamethoxazole photocatalytic ozonation in water, Water Res. 43 (2009) 1359–1369.
[41] P. Calza, V.A. Sakkas, C. Medana, C. Baiocchi, A. Dimou, E. Pelizzetti, T. Albanis, Photocatalytic degradation study of diclofenac over aqueous TiO_2 suspensions, Appl. Catal. B: Environ. 67 (2006) 197–205.
[42] P.Y. Zhang, J. Liu, Photocatalytic degradation of trace hexane in the gas phase with and without ozone addition: kinetic study, J. Photochem. Photobiol. A: Chem. 167 (2004) 87–94.